Electronic Supplementary Material (ESI) for Chemical Communications.


# Supplementary Information

## Adaptation of Thermophilic Acetyltransferase to Water-mediated Catalytic Mechanism

**Yu-Yung Chang[1], Sora Hagawa[2], and Chun-Hua Hsu[1,3,*]**

[1]Department of Agricultural Chemistry, National Taiwan University, Taipei 10617, Taiwan

[2]Institute of Molecular and Cellular Biology, National Taiwan University, Taipei 10617, Taiwan

[3]Institute of Biochemical Sciences, National Taiwan University, Taipei 10617, Taiwan

* Corresponding author:

Chun-Hua Hsu

E-mail: andyhsu@ntu.edu.tw

**In Brief**

Generally, the kinetic energy of molecules increases at higher temperature, so the backbone and side chains of the protein fluctuate and rotate more freely; thus, distances between catalytic residues may increase. However, with SsArd1, the distance between two residues did not change much with increasing temperature, from 338 to 373 K. By mutating either of the catalytic residues to Ala, the data from MD simulation suggest that both residues co-stabilized each other and also affected how water could interact with the remaining residue. With decreasing number of hydrogen bonds between water and catalytic residues, the residues had less force to "trap" the water molecule for catalytic purposes. Co-stabilizing both residues even with increasing temperature might also help the "water-trapping" between both residues, which was beneficial to retaining catalytic performance at higher temperature. In the same way, the mutant with two catalytic residues exchanged had similar catalytic performance as wild-type SsArd1 by maintaining "water-trapping" ability and possibility.

## Experimental Section

### Protein expression and purification

The open reading frame coding for SsArd1 was cloned by PCR from *Sulfolobus solfataricus* genomic DNA into the pET28a expression vector. The site-directed mutagenesis followed the manufacturer's protocol (QuickChange, stratagene) with pET28a-SsArd1 used as a template. The overexpressed recombinant protein of the wild type and mutants contained 6xHis-tag at the C-terminus. Overexpression of recombinant proteins were produced in *Escherichia coli* strain BL21 (DE3) grown in LB broth medium supplemented with 100 μg $ml^{-1}$ kanamycin and induced with 1.0 mM isopropyl 1-thio-β-D-galactopyranoside (IPTG) at 37 $^{o}$C until optical density (OD) ~0.6 for 4 h. The cultured cells were pelleted by centrifugation, suspended in buffer A (20 mM Tris-HCl, pH 8.0, 100 mM NaCl, 1 mM DTT) and lysed by sonication on ice. The insoluble pellets were removed by centrifugation at 18,000 g for 30 min at 4 $^{o}$C. Before loading into $Ni^{2+}$-affinity column, the supernatant was filtered through a 0.45-μ filter. The column was washed with buffer A containing 150 mM imidazole and eluted with buffer A containing 300 mM imidazole. To obtain higher purity, the eluted fractions were further purified by size-exclusion chromatography on a HiPrep 16/60 Sephacryl S-200 HR column (GE Healthcare) with buffer B (20 mM Tris-HCl, pH 8.0, 200 mM NaCl, 1 mM DTT). The purity of purified protein was monitored by 15% SDS-PAGE. The proteins were dialyzed against buffer A and concentrated by ultrafiltration by using Vivaspin 20 (Sartorius).

### Crystallization and data collection

H88A/E127A and H88E/E127H mutated proteins were concentrated to 6 mg $ml^{-1}$ for crystallization screening with the commercial screening kits Crystal Screen, Crystal Screen 2, PEGRx1, PEGRx1, PEG/Ion, PEG/Ion 2, SaltRx1, SaltRx2, Natrix and Index (Hampton Research); MD1-13 (Molecular Dimensions); Wizard I and Wizard II (Rigaku Reagents) in a 96-well plate at 283 K. Crystals of the SsArd1 H88A/E127A double mutant were grown by sitting drop vapour diffusion against reservoir solution containing 0.75 M ammonium sulfate, 0.1 M sodium acetate trihydrate, pH 4.2 and 0.1 M lithium sulfate. For the H88E/E127H double mutant, a single crystal was grown by sitting drop vapour diffusion against reservoir solution containing 20 % Tacsimate, pH 7.0. The crystals were transferred to harvest solution containing well solution supplemented with 25% and 20% glycerol before flash-freezing to nitrogen-gas stream.

X-ray diffraction and data collection were performed at 100 K on a SPXF beamline BL13B1 and BL13C1 of the National Synchrotron Radiation Research Center (NSRRC, Hsinchu, Taiwan), and the dataset was processed and scaled with HKL2000.[1]

**Structure determination and refinement**

The initial phases of H88A/E127A and H88E/E127H SsArd1 mutants were obtained by molecular replacement with the Phaser program[2] in the PHENIX system[3] by using the crystal structure of SsArd1 (PDB ID: 4R3K)[4] as a search model. The model building and refinements involved the program Coot[5] and phenix.refine, respectively. Water molecules were introduced if peaks > 3.0 σ in the (Fo-Fc) electron density map were in the range of a hydrogen bond. The geometric parameters of the final models were checked by using PROCHECK[6] and MolProbity.[7]

**Circular dichroism (CD) spectroscopy**

The secondary structure and melting point curve of wild-type and various SsArd1 mutants were monitored by using a Jasco J-810 spectropolarimeter equipped with a Peltier effect temperature controller (Jasco PTC-423S). For CD experiments, purified protein samples were dialyzed against 20 mM phosphate buffer (pH 8.0) and 2 mM NaCl. The far-UV spectra (195-260) were acquired with a 50-μM concentration of the wild type and all mutants. The parameters of scanning speed, data patch, band width, response time and sensitivity were set to 50 nm $min^{-1}$, 0.5 nm, 1 nm, 1 s and 100 mdeg, respectively. The thermal denaturation was performed at 220 nm with a 1°C/min increment rate of temperature from 25-95°C. Three consecutive scans were accumulated, and averaged spectra represented final spectra.

**Enzyme kinetic measurements**

The 50-μL reaction mixture contained 2 μM enzyme solution (20 mM Tris-HCl, pH 8.0, 100 mM NaCl, 1 mM EDTA), substrate solution (20 mM Tris-HCl, pH 8.0, 100 mM NaCl, 1 mM EDTA and 200 μM Alba1) and 1 mM acetyl-CoA (20 mM Tris-HCl, pH 8.0, 100 mM NaCl, 1 mM EDTA).

For enzyme kinetic assay, the 50-μL reaction mixture contained 2 μM enzyme solution (20 mM Tris-HCl, pH 8.0, 100 mM NaCl, 1 mM EDTA), substrate solution (20 mM Tris-HCl, pH 8.0, 100 mM NaCl, 1 mM EDTA and variable concentrations of peptide substrate) and 1 mM acetyl-CoA (20 mM Tris-HCl, pH 8.0, 100 mM NaCl, 1 mM EDTA). The reaction mixture was incubated at 25 and 65°C for 10 min and stopped by

adding 50 μL stop solution (20 mM Tris-HCl, pH 8.0, 100 mM NaCl, 8 M Urea). Then, 100 μL Ellman's reagent (20 mM Tris-HCl, pH 8.0, 100 mM NaCl, 1 mM EDTA and 2 mM DTNB) was added for incubation at 25°C for 10 min. The absorbance values were recorded at wavelength 412 nm on a 96-well plate. The 50-μL standard concentration of CoA (20 μM to 400 μM) was reacted with 50-μL stop solution and 100 μL Ellman's reagent. The raw data were fitted to a Michaelis-Menten equation in SigmaPlot to obtain the steady-state kinetic parameters. Three N-terminal 6-mer peptides for enzyme assays were synthesized and named Alba (SSGTPT), derived from native substrate proteins Alba. All enzyme kinetic assay was carried out three experiment repeats.

**Molecular dynamics (MD) simulation**

The crystal structure of SsArd1 (PDB ID: 4R3K)[4] was used for MD simulations with GROMACS v5.1.3.[8] The molecular topology of protein was created according to the parameters from the GROMOS96 43a1 force field, and the coordinate of the protein was placed in a dodecahedral box solvated with water molecules parameterized according to the SPC3 water model. $Na^+$ and $Cl^-$ ions were added to the solution to neutralize the net charge of the complex and reach an ionic strength of 0.15 M. The system was then energy-minimized by using a steep descent algorithm with an initial step size of 0.01 nm for 50000 steps or when the maximum force converged below 1000 kJ $mol^{-1}nm^{-1}$, followed by100 ps NVT equilibrations with cut-off distance 1.0 nm for both electrostatic and van der Waals force. Initial kinetic energies of atoms were generated by Maxwell speed distribution and assigned randomly. After NVT equilibrations, 100 ps NPT equilibrations were continued with the Parrinello-Rahman algorithm for pressure coupling. Various MD simulations were run for wild-type SsArd1 and mutants at target temperatures of 298, 338 and 373. All productive MD simulations had a 2-fs time step, 500000000 steps for a total of 100 ns each; snapshots were taken every 10 ps. The collected trajectory was then analyzed by using GROMACS or VMD 1.9.2.

**Table S1. Analysis of catalytic residues from SsArd1 and other GNATs with known structure in the mechanism of water-mediated catalysis.**

| Protein | PDB | Catalytic residues |
|---|---|---|
| SsArd1 | 4R3K | His88 Glu127 |
| hNaa50p | 3TFY | Tyr73 His112 |
| RimI | 2CNS | Glu103 |
| tGCN5 | 1QSN | Glu122 |

**Table S2.** X-ray crystallographic data collection and refinement statistics for SsArd1 H88A/E127A and H88E/E127H mutants

| Crystal parameters | 6AG4 | 6AG5 |
|---|---|---|
| Crystal | SsArd1 H88A/E127A | SsArd1 H88E/E127H |
| Space Group | $P2_12_12_1$ | $P2_12_12_1$ |
| Unit Cell Parameters | | |
| a, b, c (Å) | 42.3; 53.1; 74.5 | 41.2; 52.9; 73.6 |
| α,β,γ (°) | 90, 90, 90 | 90, 90, 90 |
| Monomers per Asymmetric Unit Cell | 1 | 1 |
| Data collection | | |
| Wavelength (Å) | 1.00 | 0.9765 |
| Resolution Range (Å) | 28.0-2.26 (2.34-2.26) | 21.31-2.32 (2.40-2.32) |
| Unique Reflections | 8167 | 7313 |
| I/σ | 24.6 (10.8) | 10.7(4.8) |
| $R_{merge}$[a,b] (%) | 4.9 (15.2) | 17.8 (39.4) |
| Completeness[a] (%) | 97.8 (88.3) | 99.5 (95.0) |
| Redundancy[a] | 4.9 (4.7) | 6.3 (4.5) |
| Refinement statistics | | |
| Resolution (Å) | 2.26 | 2.32 |
| $R_{work}$ (%) / $R_{free}$ (%)[c] | 16.3/ 22.9 | 16.0/24.9 |
| R.M.S.D. | | |
| Bonds (Å) | 0.007 | 0.008 |
| Angles (°) | 1.02 | 1.19 |
| Mean B-factor (Å$^2$) | | |
| Protein | 35.4 | 25.2 |
| CoA | 47.3 | 32.5 |
| Water | 41.9 | 29.6 |
| Ramachandran plot (%) | | |
| Favored | 99.3 | 99.0 |
| Allowed | 0.7 | 1.0 |
| Outliers | 0.0 | 0.0 |

[a] Values in parentheses are for the highest resolution shell.

[b] $R_{merge}=\Sigma_h\Sigma_i|I_{h,i}-I_h|/\Sigma_h\Sigma_i I_{h,i}$, where $I_h$ is the mean intensity of the $i$ observations of symmetry-related reflections of $h$.

[c] $R_{work}/R_{free}=\Sigma|F_{obs}-F_{calc}|/\Sigma F_{obs}$, where $F_{calc}$ is the calculated protein structure factor from the atomic model ($R_{free}$ was calculated with 5% of the reflections selected).

**Table S3.** Effect of temperature on reaction rates and kinetic parameters of wild-type (WT) SsArd1 and mutants

| | WT | H88A | E127A | H88A/E127A | H88E/E127H |
|---|---|---|---|---|---|
| °C | | | $k_{cat}$ ($min^{-1}$) | | |
| 25 | 3.69 ± 0.27 | 3.59 ± 0.21 | 3.48 ± 0.19 | N.D | 3.39 ± 0.25 |
| 35 | 6.31 ± 0.79 | 4.88 ± 0.36 | 3.81 ± 0.21 | N.D | 5.46 ± 0.39 |
| 45 | 12.46 ± 1.67 | 6.04 ± 0.60 | 5.64 ± 0.42 | N.D | 11.05 ± 1.00 |
| 55 | 21.35 ± 1.27 | 5.81 ± 0.51 | 6.38 ± 0.59 | N.D | 20.33 ± 1.34 |
| 65 | 25.45 ± 0.78 | 9.28 ± 1.05 | 8.20 ± 0.97 | N.D | 24.27 ± 1.44 |
| °C | | | $K_m$ (μM) | | |
| 25 | 146.60 ± 30.88 | 44.75 ± 10.45 | 42.87 ± 9.70 | N.D | 146.60 ± 31.71 |
| 35 | 143.50 ± 52.54 | 41.08 ± 12.30 | 47.55 ± 10.43 | N.D | 95.43 ± 22.22 |
| 45 | 256.00 ± 83.70 | 85.25 ± 28.87 | 45.95 ± 13.84 | N.D | 230.70 ± 52.96 |
| 55 | 319.60 ± 43.14 | 109.60 ± 31.05 | 50.21 ± 18.06 | N.D | 341.90 ± 50.26 |
| 65 | 336.90 ± 23.22 | 317.60 ± 82.12 | 304.80 ± 83.37 | N.D | 319.60 ± 43.14 |
| °C | | | $k_{cat}$ / $K_m$ (1/min·μM) | | |
| 25 | 2.52 x $10^{-2}$ | 8.02 x $10^{-2}$ | 8.12 x $10^{-2}$ | N.D | 2.31 x $10^{-2}$ |
| 35 | 4.40 x $10^{-2}$ | 11.88 x $10^{-2}$ | 8.01 x $10^{-2}$ | N.D | 5.72 x $10^{-2}$ |
| 45 | 4.87 x $10^{-2}$ | 7.09 x $10^{-2}$ | 12.30 x $10^{-2}$ | N.D | 4.80 x $10^{-2}$ |
| 55 | 6.68 x $10^{-2}$ | 5.30 x $10^{-2}$ | 12.71 x $10^{-2}$ | N.D | 5.95 x $10^{-2}$ |
| 65 | 7.55 x $10^{-2}$ | 2.92 x $10^{-2}$ | 2.69 x $10^{-2}$ | N.D | 7.59 x $10^{-2}$ |

**Table S4.** Mean number of water H-bonds formed with catalytic residues from the MD simulation

| Mean number of water H-bonds (within 4 Å of residue 127) with residue 88 | | | | |
|---|---|---|---|---|
| | WT | H88A | E127A | H88E/E127H |
| 298K | 0.001996 | 0 | 0.251497 | 1.406504 |
| 338K | 0.061876 | 0 | 0.083832 | 0.916908 |
| Mean number of water H-bonds (within 4 Å of residue 88) with residue 127 | | | | |
| | WT | H88A | E127A | H88E/E127H |
| 298K | 2.335329 | 0.922156 | 0.325349 | 0.384824 |
| 338K | 1.866267 | 0.309381 | 0.227545 | 0.156084 |

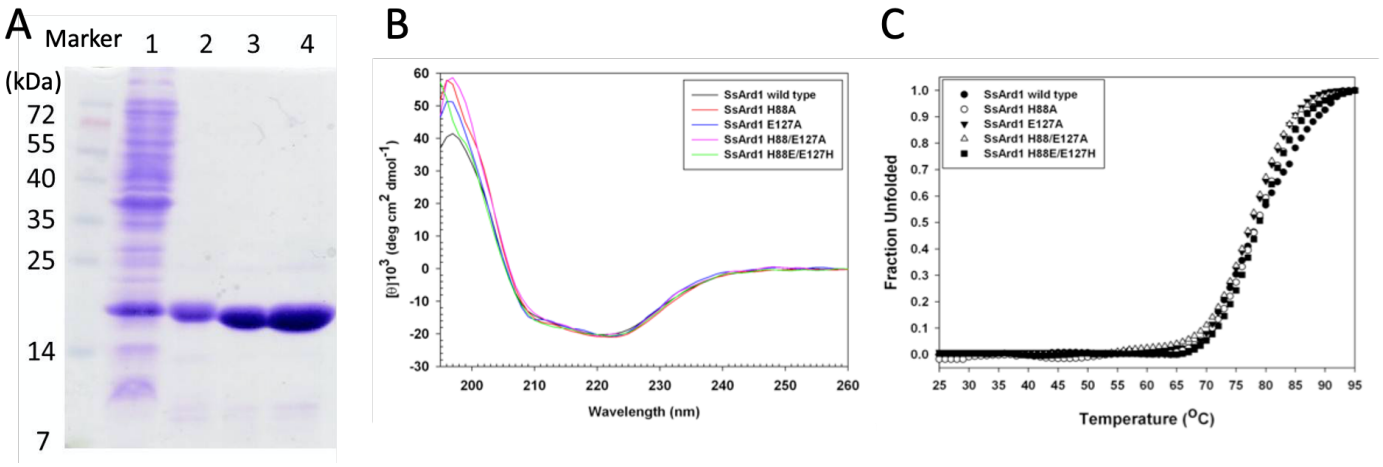


**Figure S1.** Protein production and analysis of secondary structure and thermostability by far-UV CD spectra. (A) SDS-PAGE analysis of the SsArd1 purification. Lane 1: raw lysate; Lane 2: purified protein by Ni-NTA affinity column; Lane 3: purified protein by gel filtration column; Lane 4: protein concentrated for stock. (B) Secondary structure and (C) thermostability analysis of wild-type and mutated SsArd1 by far-UV circular dichroism spectra

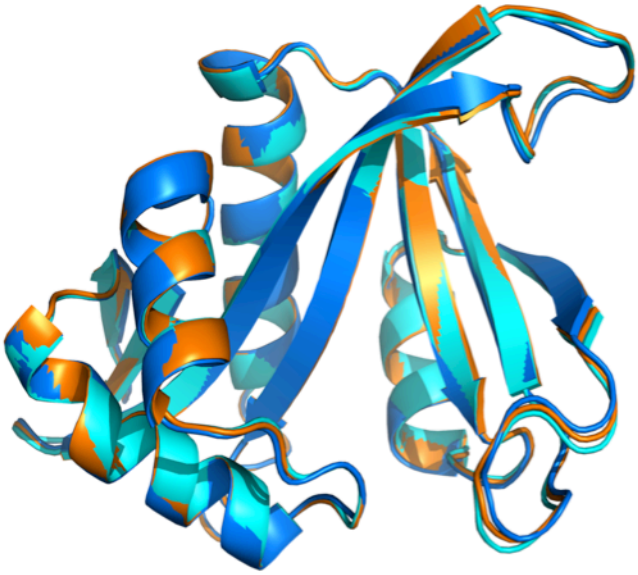

**Figure S2.** Structural alignment of wild-type (blue), H88A/E127A (orange) and H88E/E127H (cyan)-mutated SsArd1.

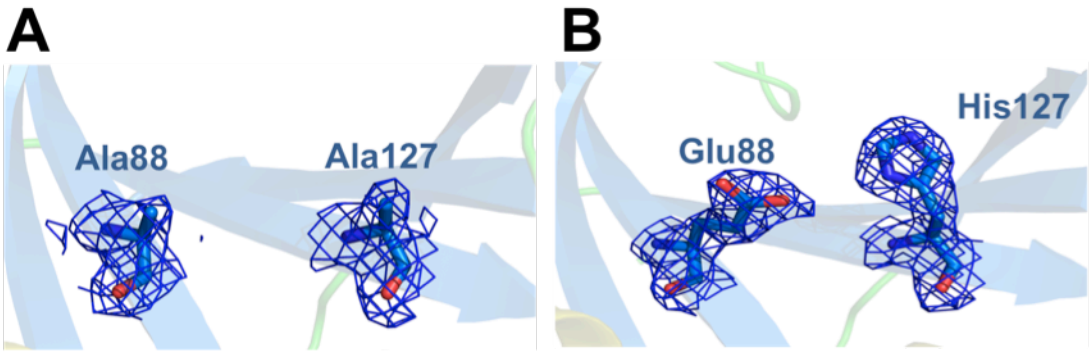


**Figure S3.** Representative of $2F_o$-$F_c$ electron density maps at 1.6σ-level of mutated active site in (A) H88A/E127A and (B) H88E/E127H mutants.

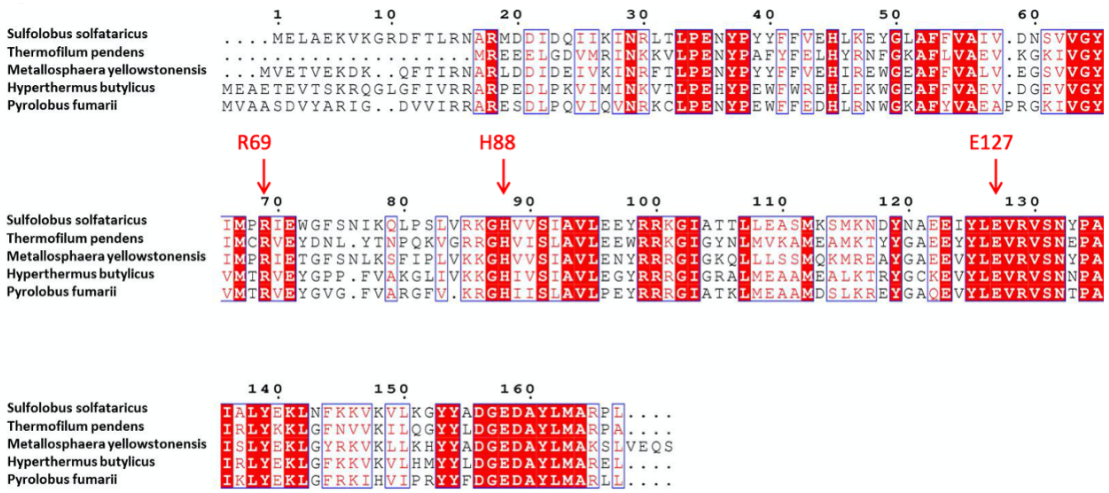


**Figure S4.** Multiple sequence alignment of SsArd1 and thermophilic homologues from *Thermofilum pendens, Metallosphaera yellowstonensis, Hyperthermus butylicus* and *Pyrolobus fumarli*. Identical and similar residues are labeled by white letters on red backgrounds and red letters, respectively.

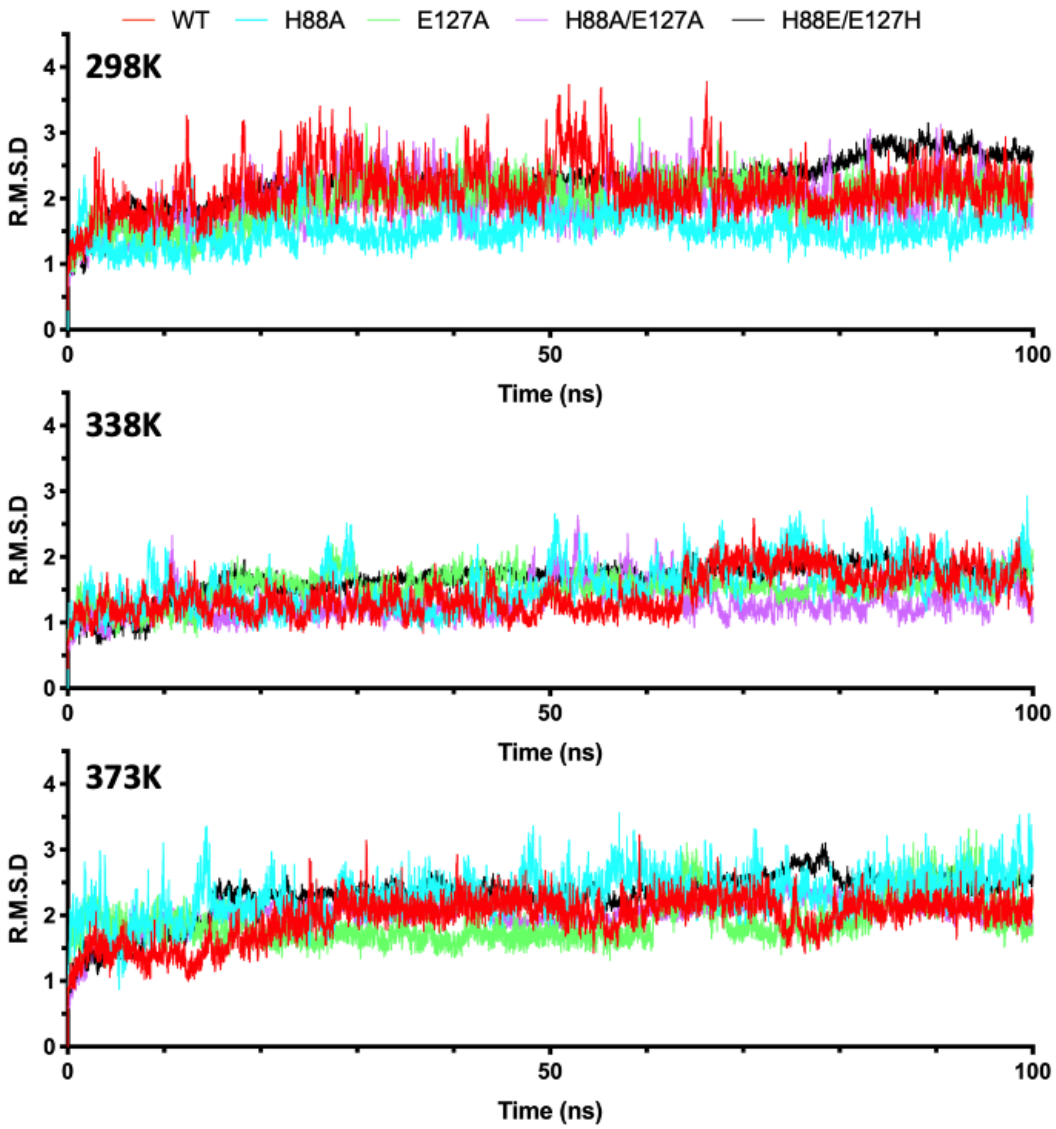


**Figure S5.** (a): Backbone RMSD comparison of WT and mutated SsArd1 throughout simulation at 298 K (upper), 338K (middle) and 373K (lower).

**References**


1. Z. Otwinowski and W. Minor, in *Methods in Enzymology*, ed. Charles W. Carter, Jr., Academic Press, 1997, vol. Volume 276, pp. 307-326.
2. A. J. McCoy, R. W. Grosse-Kunstleve, P. D. Adams, M. D. Winn, L. C. Storoni and R. J. Read, *J Appl Crystallogr*, 2007, **40**, 658-674.
3. P. D. Adams, P. V. Afonine, G. Bunkoczi, V. B. Chen, I. W. Davis, N. Echols, J. J. Headd, L. W. Hung, G. J. Kapral, R. W. Grosse-Kunstleve, A. J. McCoy, N. W. Moriarty, R. Oeffner, R. J. Read, D. C. Richardson, J. S. Richardson, T. C. Terwilliger and P. H. Zwart, *Acta Crystallogr D Biol Crystallogr*, 2010, **66**, 213-221.
4. Y. Y. Chang and C. H. Hsu, *Sci Rep*, 2015, **5**, 8673.
5. P. Emsley, B. Lohkamp, W. G. Scott and K. Cowtan, *Acta Crystallogr D Biol Crystallogr*, 2010, **66**, 486-501.
6. R. A. Laskowski, M. W. MacArthur, D. S. Moss and J. M. Thornton, *Journal of Applied Crystallography* 1993, **26**, 283-291.
7. V. B. Chen, W. B. Arendall, 3rd, J. J. Headd, D. A. Keedy, R. M. Immormino, G. J. Kapral, L. W. Murray, J. S. Richardson and D. C. Richardson, *Acta Crystallogr D Biol Crystallogr*, 2010, **66**, 12-21.
8. D. Van Der Spoel, E. Lindahl, B. Hess, G. Groenhof, A. E. Mark and H. J. Berendsen, *J Comput Chem*, 2005, **26**, 1701-1718.